Spin-rotational-invariant theory of transition-metal magnetism at finite temperatures: Systematic study of a single-site model

G. M. Pastor
Institut für Theoretische Physik, Universität Kassel, Heinrich Plett Strasse 40, 34132 Kassel, Germany

J. Dorantes-Dávila
Instituto de Física, Universidad Autónoma de San Luis Potosí, Alvaro Obregón 64, 78000 San Luis Potosí, Mexico

(Received 3 March 2016; published 27 June 2016)

A spin-rotational-invariant approach to the spin-fluctuation theory of itinerant-electron magnetism is proposed and evaluated in the framework of a d-band model Hamiltonian including intra-atomic exchange interactions J and the coupling to a local magnetic field B. Using a vector-field Hubbard-Stratonovich transformation, we obtain a static approximation to the density matrix operator from which the equilibrium properties are directly derived. The method is applied to a single-site model taking Fe as a representative example. Exact and approximate analytical results are given for the local magnetic moments, their longitudinal and transversal components, the field-induced magnetizations, entropy, and heat capacity. Goals and limitations of various approximations are discussed as a function of J, B, and temperature. The quantum-mechanical origin of some important drawbacks found in previous vector-field static approaches is identified. The significant improvements achieved with the static density operator are demonstrated.

DOI: 10.1103/PhysRevB.93.214435

I. INTRODUCTION

Magnetic materials based on transition metals and their compounds define one of the most active research areas in condensed-matter physics. Technological applications, ranging from metallurgy, over high-density recording media, to spin electronics, are certainly a major driving force in this field [1–8]. Furthermore, understanding and controlling itinerant-electron magnetism at a microscopic level represents a particularly important and challenging open problem from a fundamental perspective. Recent experimental progress has opened the way to manipulation and characterization techniques at extraordinary levels of spatial and temporal resolution [6–9]. These advances motivate and indeed benefit from the continuous development of first-principles and model theoretical investigations [10,11].

From the point of view of theory, the subtle interplay between environment-dependent electronic structure, correlations, spin-orbit interactions, and magnetic excitations poses a remarkable difficulty, especially at finite temperatures. In past years, a large number of theoretical studies have been performed by using spin models at different levels of approximation [12–17], exact numerical solutions of simple electronic models [18], and realistic electronic structure approaches [19–29]. From the latter perspective, most finite-temperature calculations on itinerant-electron magnetism involve treating Coulomb interactions in broken spin-symmetry approximations, where the spin-polarized density and its fluctuations are assumed to be collinear. However, rotational-invariant methods are currently attracting increasing attention since they give access to more complex forms of magnetic order and excitations. This is fueled by several factors. First, a variety of stable noncollinear ground-state magnetic structures has been observed, particularly in transition-metal (TM) nanostructures [17,30–39]. The physics behind these phenomena is far from obvious and deserves a specific theoretical description [40–43]. Second, many-body rotational-invariant theories are important in order to rigorously understand the effects of spin-orbit interactions since they remove precisely this symmetry, thereby leading to magnetic anisotropy and some degree of noncollinearity [8,44]. Finally, transversal spin excitations are expected to be important for describing the finite-temperature behavior [45–48], as well as the magnetization dynamics triggered by external optical or electron-injection pulses [9,11].

Several studies have been performed by taking into account spin excitations beyond collinear approximations [49–52]. Hubbard already considered randomized vector exchange fields by using a model expression for the energy associated with each exchange-field configuration [49]. Uchida and Kakehashi studied amorphous transition-metal systems within a noncollinear two-field functional-integral method, in which transversal spin fluctuations were neglected [53]. Lavrentiev *et al.* combined a cluster expansion with kinetic Monte Carlo simulations, including noncollinear arrangements of the spin degrees of freedom [17]. In this way, they investigated the effects of temperature on the energy and magnetic order at the interfaces of Fe-Cr alloys. Furthermore, a dynamical spin-fluctuation theory of narrowband itinerant electrons has been proposed by using functional-integral methods and the single-site coherent potential approximation [45–47]. More recently, the role of transversal spin fluctuations and their consequences on the Curie temperature of Fe have been studied in the framework of a static virtual crystal approximation [48]. However, despite the obvious interest of incorporating the transversal spin fluctuations in the finite-temperature theory, the reputation of the vector-field functional approach has been tarnished by some serious limitations in the atomic limit. Indeed, as shown by Kakehashi [54], the vector-field static approximation yields a negative specific heat and a diverging entropy in the atomic limit at low temperatures. These drawbacks can hardly be overlooked in the long run, particularly since in TMs the dominant Coulomb interactions,

 ©2016 American Physical Society

and an important part of the electronic correlations, have local roots. It is therefore important to understand the source of these inaccuracies in more detail, and to find sound alternative routes to the development of noncollinear spin-fluctuation theory.

The main purpose of this paper is to introduce a simple spin-rotational-invariant approach to the finite-temperature magnetic properties of transition metals, which incorporates the fluctuations of the transversal spin degrees of freedom, and to demonstrate its accuracy by comparison with exact results. The method is based on a static approximation to the equilibrium density matrix operator $\hat{\rho}$. The thermodynamic properties are directly obtained from the statistical average of the corresponding operators since the usual thermodynamic relations involving derivatives of the logarithm of the partition function Z cannot be taken for granted. In this way, we avoid unnecessary violations of the commutation rules between the spin operators, which are indeed responsible for the drawbacks of previous noncollinear theories [54]. An exactly solvable single-site model of $3d$-electron magnetism is investigated systematically in order to validate our theory. Exact and approximate results for a number of observables are analyzed as a function of temperature T and local magnetic field B. In this way, the very good accuracy of the present approach is demonstrated.

The remainder of the paper is organized as follows. In Sec. II, the single-site model is presented and its equilibrium properties are derived both exactly and in the vector-field static approximation. The origin of the potential shortcomings of the latter is identified and the static density operator is introduced. The thermodynamic properties predicted by the different approaches are reported and contrasted in Sec. III. Goals and limitations of the static approximation are discussed in a broad range of parameters, including isotropic and anisotropic cases. The improvements achieved with the static density operator are quantified. Finally, Sec. IV summarizes the main conclusions and points out some important future perspectives.

II. THEORY

In this section, we determine the finite-temperature properties of the valence $3d$ electrons by considering the atomic limit of a spin-rotational-invariant Hamiltonian. Once the model is presented and its parameters defined, we determine its finite-temperature properties exactly in the canonical ensemble. The problem is then solved by using a vector-field functional-integral method in the static approximation which, in contrast to the exact solution, is universally applicable. Although the decoupling scheme preserves the rotational symmetry of the Hamiltonian, the static approximation does not respect the commutation rules between the spin-operator components. The consequences are quantified by contrasting the properties derived from the static partition function $Z_{\rm st}$ with the exact solution. The relation between the derivatives of $Z_{\rm st}$ and the physical observables is analyzed from the perspective of operator algebra. This brings us to propose a direct averaging scheme based on the static density operator $\hat{\rho}_{\rm st}$, which is shown to remove all major limitations of $Z_{\rm st}$ and to systematically improve the quality of the static approximation.

A. Single-site model

We consider the d-band model Hamiltonian $\hat{H}$ proposed in Ref. [48] in the atomic limit, i.e., for vanishing hopping integrals. Setting the d-orbital energies equal to zero, the single-particle term in $\hat{H}$ vanishes. Since there are no charge fluctuations in the absence of hopping, we consider a constant number of electrons, $n_d = 7$, corresponding to Fe, and refer all energies to the direct Coulomb energy $NUn_d(n_d-1)/2$, where U refers to the intra-atomic direct Coulomb integral and N to the number of atoms [48]. Taking into account the interaction with an external magnetic field or local anisotropy field $\vec{B}$, the model takes the form

$$\hat{H} = -J\sum_l (\hat{\vec{S}}_l \cdot \hat{\vec{S}}_l - 2\vec{B}\cdot\hat{\vec{S}}_l), \tag{1}$$

where J is the intra-atomic Coulomb exchange integral and $\hat{\vec{S}}_l$ the spin operator at atom l. Throughout the paper, we measure B in the same units as J by incorporating in B the Bohr magneton $\mu_B = 5.8\times10^{-5}$ eV/T. Since $\hat{H}$ splits in a sum over all the atoms in the lattice, we may consider a single atom and drop the index l, keeping in mind that all properties are referred to one atom. We thus obtain the single-site model

$$\hat{H} = -J\hat{S}^2 - 2B\hat{S}_z, \tag{2}$$

where $\hat{S}^2 = \hat{S}_x^2 + \hat{S}_y^2 + \hat{S}_z^2$, and the magnetic field $\vec{B} = B\hat{z}$ points along the z axis.

B. Exact solution

In order to obtain the exact canonical partition function $Z = \mathrm{Tr}\{e^{-\beta\hat{H}}\}$, where $\beta = 1/k_{\rm B}T$, and the free energy $F = -k_{\rm B}T\ln(Z)$, we observe that for $n_d = 7$ electrons in a d shell, there are 10 states with $S = 3/2$ and 40 states with $S = 1/2$. It is then straightforward to calculate the trace in the $S = 3/2$ and $1/2$ subspaces using the basis with well-defined S and S_z. The result is [55]

$$Z = 20\, e^{\frac{15J}{4T}}\left[(1+4e^{-\frac{3J}{T}})\cosh\left(\frac{B}{T}\right) + \cosh\left(\frac{3B}{T}\right)\right], \tag{3}$$

where T incorporates the Boltzmann constant $k_{\rm B} = 8.6\times10^{-5}$ eV/K and thus has energy units like J. The thermodynamic properties of interest are obtained from the corresponding derivatives of F; for example, the spin magnetization along the field,

$$\langle\hat{S}_z\rangle = -\frac{1}{2}\frac{\partial F}{\partial B} = \frac{\sinh\left(\frac{B}{T}\right)\left\{e^{\frac{3J}{T}}\left[3\cosh\left(\frac{2B}{T}\right)+2\right]+2\right\}}{e^{\frac{3J}{T}}\left[\cosh\left(\frac{B}{T}\right)+\cosh\left(\frac{3B}{T}\right)\right]+4\cosh\left(\frac{B}{T}\right)}, \tag{4}$$

the local spin moment,

$$\langle\hat{S}^2\rangle = -\frac{\partial F}{\partial J} = \frac{15}{4} - \frac{6}{e^{\frac{3J}{T}}\cosh\left(\frac{2B}{T}\right)+2}, \tag{5}$$

the z component of the local moment,

$$\langle\hat{S}_z^2\rangle = -\frac{T}{4}\frac{\partial^2 F_{\rm st}}{\partial B^2} + \langle\hat{S}_z\rangle^2 = \frac{9}{4} - \frac{e^{\frac{3J}{T}}+4}{e^{\frac{3J}{T}}\cosh\left(\frac{2B}{T}\right)+2}, \tag{6}$$

the entropy,

$$S = -\frac{\partial F}{\partial T} = -\frac{15J}{4T} + \ln\left\{40\, e^{\frac{3J}{4T}} \cosh\left(\frac{B}{T}\right)\left[e^{\frac{3J}{T}} \cosh\left(\frac{2B}{T}\right) + 2\right]\right\} + \frac{6J - 2B\, e^{\frac{3J}{T}} \sinh\left(\frac{2B}{T}\right)}{T\, e^{\frac{3J}{T}} \cosh\left(\frac{2B}{T}\right) + 2T} - \frac{B \tanh\left(\frac{B}{T}\right)}{T}, \tag{7}$$

and the heat capacity,

$$C = -T\frac{\partial^2 F}{\partial T^2} = \frac{2\, e^{\frac{3J}{T}}\left[B^2\left(e^{\frac{3J}{T}} + 4\right) + 9J^2\right]\cosh\left(\frac{2B}{T}\right) + B\left\{2B\, e^{\frac{6J}{T}} + 8\, e^{\frac{3J}{T}}\left[3J \sinh\left(\frac{2B}{T}\right) + B\right] + B\left(e^{\frac{3J}{T}} - 2\right)^2 \mathrm{sech}^2\left(\frac{B}{T}\right)\right\}}{T^2\left[e^{\frac{3J}{T}} \cosh\left(\frac{2B}{T}\right) + 2\right]^2}. \tag{8}$$

C. Functional integral method in the static approximation

In order to obtain the partition function Z_{st} in the static approximation, we first linearize the operators S_α^2 with $\alpha = x$, y, and z in the exponential of $\hat{H}$ by means of a Hubbard-Stratonovich transformation [56]. An exchange field ξ_α is thereby introduced for each Cartesian component $\hat{\vec{S}}$, usually gathered in the local exchange vector field $\vec{\xi}$. Since the different $\hat{S}_\alpha^2$ do not commute with each other, $\vec{\xi}$ depends on Feyman's "time" or ordering parameter [57]. However, the static approximation neglects this "time" dependence, which in the present case amounts to ignoring the noncommutativity of the $\hat{S}_\alpha$. In this way, one obtains

$$Z_{\mathrm{st}} = \left(\frac{\beta J}{4\pi}\right)^{3/2} \int e^{-\frac{\beta J}{4}\xi^2} \mathrm{Tr}\{e^{-\beta \hat{H}'(\vec{\xi})}\}\, d\vec{\xi}, \tag{9}$$

where $\xi^2 = \xi_x^2 + \xi_y^2 + \xi_z^2$ and

$$\hat{H}'(\vec{\xi}) = -J\vec{\xi} \cdot \vec{S} - 2BS_z. \tag{10}$$

The trace in Eq. (9) can be obtained straightforwardly by choosing the spin quantization direction along $J\vec{\xi} - 2\vec{B}$ [see Eq. (10)]. Integration over all $\vec{\xi}$ yields [55]

$$Z_{\mathrm{st}} = 10\, e^{\frac{J}{4T}}\left\{\frac{5J}{B}\sinh\left(\frac{B}{T}\right) + 10\cosh\left(\frac{B}{T}\right) + e^{\frac{2J}{T}}\left[\frac{3J}{B}\sinh\left(\frac{3B}{T}\right) + 2\cosh\left(\frac{3B}{T}\right)\right]\right\}. \tag{11}$$

The usual procedure in previous approaches using the static approximation has been to obtain the thermodynamic properties from the approximate free energy $F_{\mathrm{st}} = -k_{\mathrm{B}}T \ln(Z_{\mathrm{st}})$, by taking the corresponding partial derivatives [48,54]. It should be noted, however, that this most often implies additional approximations, beyond the static assumption at the Hubbard-Stratonovich level, which can lead to serious drawbacks. This can actually be avoided by performing the averages in a well-defined static mixed state, as will be shown in Sec. II D.

Partial derivation of F_{st} yields the following approximations to the spin magnetization along the magnetic field

$$\langle \hat{S}_z \rangle = -\frac{1}{2}\frac{\partial F_{\mathrm{st}}}{\partial B} = \frac{(2B^2 - JT)\left[3\, e^{\frac{2J}{T}} \sinh\left(\frac{3B}{T}\right) + 5\sinh\left(\frac{B}{T}\right)\right] + BJ\left[9\, e^{\frac{2J}{T}} \cosh\left(\frac{3B}{T}\right) + 5\cosh\left(\frac{B}{T}\right)\right]}{2B\left\{5J\sinh\left(\frac{B}{T}\right) + e^{\frac{2J}{T}}\left[3J\sinh\left(\frac{3B}{T}\right) + 2B\cosh\left(\frac{3B}{T}\right)\right] + 10B\cosh\left(\frac{B}{T}\right)\right\}}, \tag{12}$$

the local spin moment,

$$\langle \hat{S}^2 \rangle = -\frac{\partial F_{\mathrm{st}}}{\partial J} = \frac{9}{4} + \frac{5(T - 2J)\sinh\left(\frac{B}{T}\right) + 3T\, e^{\frac{2J}{T}} \sinh\left(\frac{3B}{T}\right) - 20B\cosh\left(\frac{B}{T}\right)}{5J\sinh\left(\frac{B}{T}\right) + e^{\frac{2J}{T}}\left[3J\sinh\left(\frac{3B}{T}\right) + 2B\cosh\left(\frac{3B}{T}\right)\right] + 10B\cosh\left(\frac{B}{T}\right)}, \tag{13}$$

the longitudinal component of the local moment,

$$\langle \hat{S}_z^2 \rangle = -\frac{T}{4}\frac{\partial^2 F_{\mathrm{st}}}{\partial B^2} + \langle \hat{S}_z \rangle^2 = \frac{5J(B^2 + 2T^2)\sinh\left(\frac{B}{T}\right) + 3J\left(9B^2 + 2T^2\right)e^{\frac{2J}{T}} \sinh\left(\frac{3B}{T}\right) + 2B\left(B^2 - JT\right)\left[9\, e^{\frac{2J}{T}} \cosh\left(\frac{3B}{T}\right) + 5\cosh\left(\frac{B}{T}\right)\right]}{4B^2\left\{5J\sinh\left(\frac{B}{T}\right) + e^{\frac{2J}{T}}\left[3J\sinh\left(\frac{3B}{T}\right) + 2B\cosh\left(\frac{3B}{T}\right)\right] + 10B\cosh\left(\frac{B}{T}\right)\right\}}, \tag{14}$$

and the entropy,

$$S = -\frac{\partial F_{\mathrm{st}}}{\partial T} = \frac{J}{4T} - \frac{5(8B^2 + J^2)\sinh\left(\frac{B}{T}\right) + 3\, e^{\frac{2J}{T}}\left[(8B^2 + 9J^2)\sinh\left(\frac{3B}{T}\right) + 18BJ\cosh\left(\frac{3B}{T}\right)\right] + 30BJ\cosh\left(\frac{B}{T}\right)}{4T\left\{5J\sinh\left(\frac{B}{T}\right) + e^{\frac{2J}{T}}\left[3J\sinh\left(\frac{3B}{T}\right) + 2B\cosh\left(\frac{3B}{T}\right)\right] + 10B\cosh\left(\frac{B}{T}\right)\right\}} + \ln\left(\frac{10}{B}\left\{5J\sinh\left(\frac{B}{T}\right) + e^{\frac{2J}{T}}\left[3J\sinh\left(\frac{3B}{T}\right) + 2B\cosh\left(\frac{3B}{T}\right)\right] + 10B\cosh\left(\frac{B}{T}\right)\right\}\right). \tag{15}$$

The corresponding expression for the heat capacity,

$$C = -T\frac{\partial^2 F_{\rm st}}{\partial T^2}, \tag{16}$$

is given in the Supplemental Material [58].

It is important to recall that the static approximation ignores the commutation rules between the operators describing the interaction (e.g., $\hat{\vec{S}}_l$ and $\hat{N}_l$ in the usual local models) and the interatomic hopping terms responsible for charge fluctuations and electron delocalization. In the low-temperature limit, this leads to a mean-field treatment of Coulomb interactions, which neglects potentially important electron-correlation effects [48]. Even in the present atomic limit, where charge fluctuations are absent, the vector-field static approximation is not exact, since the spin components do not commute with each other. In fact, it has been shown [54] that in the isotropic low-temperature limit ($B = 0$ and $T \ll J$), the heat capacity predicted by Eq. (16) tends to -1 in units of $k_{\rm B}$. In Sec. III, we will show that this is not the consequence of the static treatment of noncollinear spin fluctuations, but rather of assuming that the thermodynamic properties can always be derived from $F_{\rm st}$. An alternative approach revealing the actual goals and limitations of the static approximation is presented in the following.

D. Static density operator and average properties

In order to assess the validity of Eqs. (12)–(16), it is useful to recall the operator identity

$$\frac{\partial}{\partial\lambda}e^{\hat{X}} = \int_0^1 e^{(1-\alpha)\hat{X}}\,\frac{\partial\hat{X}}{\partial\lambda}\,e^{\alpha\hat{X}}\,d\alpha, \tag{17}$$

where λ is any parameter on which $\hat{X}$ may depend. This relation, which can be easily derived by using Feynman's ordering technique [57], implies that

$$\frac{\partial}{\partial\lambda}{\rm Tr}\{e^{\hat{X}}\} = {\rm Tr}\left\{\frac{\partial\hat{X}}{\partial\lambda}\,e^{\hat{X}}\right\}, \tag{18}$$

irrespective of the commutation relation between $\hat{X}$ and $\frac{\partial\hat{X}}{\partial\lambda}$. Therefore, computing $\langle\hat{S}_z\rangle$ from $\partial F/\partial B$ as in (4) remains valid in the static approximation. However, notice that simple expressions such as (18) do not hold for the higher-order derivatives or for the derivatives of average values. In fact,

$$\frac{\partial}{\partial\lambda}\langle\hat{A}\rangle = {\rm Tr}\left\{\hat{A}\frac{\partial}{\partial\lambda}e^{\hat{X}}\right\} = \int_0^1 {\rm Tr}\left\{\hat{A}\,e^{(1-\alpha)\hat{X}}\,\frac{\partial\hat{X}}{\partial\lambda}\,e^{\alpha\hat{X}}\right\}d\alpha, \tag{19}$$

even if, as assumed, $\hat{A}$ is independent of λ. Very often, $\partial\hat{X}/\partial\lambda$ or $\hat{A}$ do not commute with $\hat{X}$. It is therefore clear that using equations such as (14) for $\langle\hat{S}_z^2\rangle$ introduces additional approximations, which are independent of the quality by which the static approximation describes the equilibrium state. Notice that this commutation problem does not appear when λ refers to the temperature T, since $\partial\hat{X}/\partial T$ is proportional to $\hat{X}$. Nevertheless, in the case of the local moment $\langle\hat{S}^2\rangle$, entropy S, and heat capacity C, one should be concerned about the physical meaning of the derivatives of $F_{\rm st} = -k_{\rm B}T\ln(Z_{\rm st})$, which can be very different from the derivatives of the exact F. This conditions the quality of $F_{\rm st}$ as a function of its various parameters. For instance, $-\partial F_{\rm st}/\partial J$ corresponds to averaging $\vec{\xi}\cdot\hat{\vec{S}}$ rather than $\hat{S}^2$, and $-(1/\beta)[\partial\ln(Z_{\rm st})/\partial\beta]$ corresponds to averaging $\hat{H}'(\vec{\xi})$ rather than $\hat{H}$ [see Eqs. (9) and (10)]. It is therefore important to keep in mind that this can also be the source of inaccuracies.

In order to circumvent these problems and make the best out of the static approximation, we take advantage of the fact that the Hubbard-Stratonovich transformation is an operator identity. Consequently, the transformation can be applied to the density operator $\hat{\rho} = e^{-\beta\hat{H}}$ in order to linearize the quadratic terms in $\hat{H}$. Introducing the static approximation in the functional integration only at this basic level, we obtain the static density operator

$$\hat{\rho}_{\rm st} = \frac{1}{Z_{\rm st}}\left(\frac{\beta J}{4\pi}\right)^{3/2}\int e^{-\beta[\hat{H}'(\vec{\xi})+\frac{J}{4}\xi^2]}\,d\vec{\xi}, \tag{20}$$

which will be used in the following to describe the equilibrium mixed state. The thermodynamic properties are thus obtained by the usual ensemble averages, namely, $\langle\hat{A}\rangle_{\rm st} = {\rm Tr}\{\hat{A}\hat{\rho}_{\rm st}\}$ for any observable $\hat{A}$.

As already discussed, averaging with $\hat{\rho}_{\rm st}$ yields Eq. (12) for $\langle\hat{S}_z\rangle_{\rm st}$. In terms of $\hat{\rho}_{\rm st}$, the local spin moment is given,

$$\langle\hat{S}^2\rangle_{\rm st} = {\rm Tr}\{\hat{S}^2\hat{\rho}_{\rm st}\} = \frac{15}{4} - \frac{12\left[J\sinh\left(\frac{B}{T}\right)+2B\cosh\left(\frac{B}{T}\right)\right]}{5\left[J\sinh\left(\frac{B}{T}\right)+2B\cosh\left(\frac{B}{T}\right)\right]+e^{\frac{2J}{T}}\left[3J\sinh\left(\frac{3B}{T}\right)+2B\cosh\left(\frac{3B}{T}\right)\right]}. \tag{21}$$

In the case of the longitudinal component of the local moment $\langle\hat{S}_z^2\rangle_{\rm st} = {\rm Tr}\{\hat{S}_z^2\hat{\rho}_{\rm st}\}$, no closed analytic expression could be found, except in the isotropic case ($B = 0$) where

$$\langle\hat{S}_z^2\rangle_{\rm st} = \frac{5}{4} - \frac{4(J+2T)}{5(J+2T)+e^{\frac{2J}{T}}(9J+2T)}. \tag{22}$$

For finite B, one obtains $\langle\hat{S}_z^2\rangle_{\rm st}$ by means of a one-dimensional numerical integration. The average energy $E = \langle\hat{H}\rangle_{\rm st} = {\rm Tr}\{\hat{H}\hat{\rho}_{\rm st}\}$ is given by

$$E = \frac{(20JT-40B^2-27J^2)\sinh\left(\frac{B}{T}\right)-3\,e^{\frac{2J}{T}}(8B^2+15J^2-4JT)\sinh\left(\frac{3B}{T}\right)-74BJ\cosh\left(\frac{B}{T}\right)-66BJ\,e^{\frac{2J}{T}}\cosh\left(\frac{3B}{T}\right)}{20J\sinh\left(\frac{B}{T}\right)+4\,e^{\frac{2J}{T}}\left[3J\sinh\left(\frac{3B}{T}\right)+2B\cosh\left(\frac{3B}{T}\right)\right]+40B\cosh\left(\frac{B}{T}\right)}, \tag{23}$$

from which the heat capacity

$$C_{\rm st} = \frac{\partial \langle \hat{H} \rangle_{\rm st}}{\partial T} \tag{24}$$

is obtained. The expression for $C_{\rm st}$ is given in the Supplemental Material [58]. Alternatively, one may derive the heat capacity from

$$C'_{\rm st} = \frac{\langle \hat{H}^2 \rangle_{\rm st} - \langle \hat{H} \rangle^2_{\rm st}}{k_B T^2}, \tag{25}$$

which for $B = 0$ is given by

$$C'_{\rm st} = \frac{36J^2(J+2T)[e^{\frac{2J}{T}}(9J+2T)+J+2T]}{[5T(J+2T)+T\,e^{\frac{2J}{T}}(9J+2T)]^2}. \tag{26}$$

For $B \neq 0$, $C'_{\rm st}$ can be calculated by means of a simple numerical integration. Comparing these two approaches with the exact results will allow us to infer the ability of the $\hat{\rho}_{\rm st}$ to describe the temperature dependence of the internal energy and its fluctuations.

The entropy $S_{\rm st}$ should be calculated directly from $S[\hat{\rho}_{\rm st}] = -k_{\rm B}\langle \ln(\hat{\rho}_{\rm st}) \rangle$, which is a well-defined property of $\hat{\rho}_{\rm st}$. However, this seems very difficult in practice since it would require one to determine the logarithm of an integral of noncommuting operators. We therefore resort to the relations $\partial S/\partial T = C/T$ and $\partial S/\partial \beta = -C/\beta$, even though, strictly speaking, they hold only for the exact equilibrium $\hat{\rho} \propto \exp(-\beta \hat{H})$. We expect this assumption to be valid, as long as $\hat{\rho}_{\rm st}$ is sufficiently close to $\hat{\rho}$. An approximation to $S_{\rm st}$ is thus obtained by numerical integration of $C_{\rm st}$ starting either from $T = 0$ or from $\beta = 0$.

One may finally note that the proposed noncollinear approach can be readily applied to large finite systems and to extended systems, since it involves quantum-mechanical averages in the framework of the single-particle operator $\hat{H}'(\vec{\xi})$, followed by a classical average with respect to the local exchange fields $\vec{\xi}$ [see Eqs. (10) and (20)].

III. RESULTS AND DISCUSSION

In this section, the finite-temperature properties of the single-site model $\hat{H}$ are presented and discussed. Goals and limitations of the previously introduced approximations to the noncollinear spin-fluctuation theory are analyzed by comparison with exact results.

A. Isotropic case

In the absence of external or local anisotropy fields $\vec{B}$, the model is spin-rotational invariant. In Fig. 1, the temperature dependence of the most relevant thermodynamic properties of the model is shown for $J = 1$ and $n_d = 7$, which corresponds to Fe. The exact local spin moment $\langle S^2 \rangle$ remains essentially at its ground-state value $S(S+1) = 15/4$ until $k_{\rm B}T$ is comparable to the exchange energy J, i.e., until the $S = 1/2$ excited states become accessible. It then decreases monotonously towards the high-temperature limit $\langle S^2 \rangle_\infty = 7/4$, in which all states are equally probable. The excitation of the low-spin states manifests itself as a rather broad peak in the heat capacity at $k_{\rm B}T \simeq J$. In this temperature range $(1/2 \leqslant T/J \leqslant 3)$, the entropy shows a crossover from the ground-state value

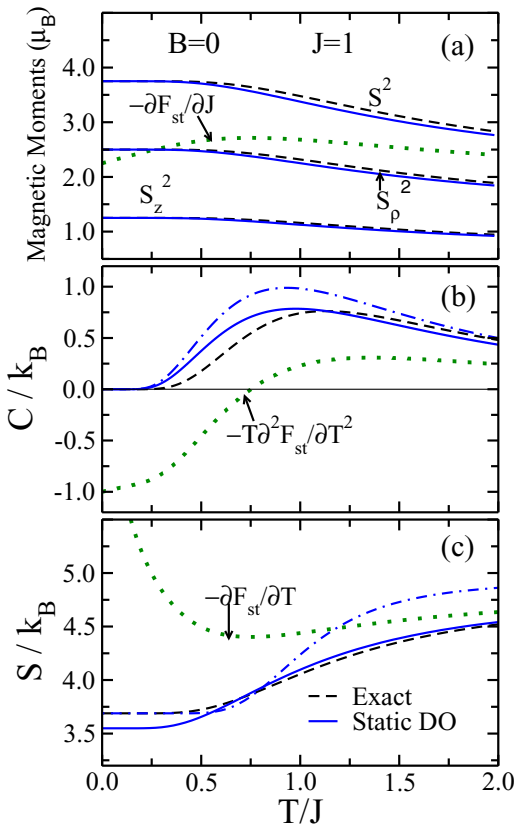

FIG. 1. Thermodynamic properties of the isotropic single-site model for $n_d = 7$ electrons: (a) Total local moment $S^2 = \langle \hat{S}^2_\rho + Sz^2 \rangle$, longitudinal component $\langle \hat{S}^2_z \rangle$, and transversal component $\langle \hat{S}^2_\rho \rangle = \langle \hat{S}^2_x + S^2_y \rangle$, (b) heat capacity C, and (c) entropy S as a function of temperature T. The full blue curves are obtained by averaging with the static density operator $\hat{\rho}_{\rm st}$ [Eq. (20)], the dashed black curves are exact results, and the dotted green curves result from the derivatives of the static free energy $F_{\rm st}$ [Eqs. (12)–(16)]. In (b), the full and dash-dotted blue curves correspond to Eqs. (24) and (26), respectively. In (c), the full (dash-dotted) blue curve is obtained by integrating $C_{\rm st}/T$ starting from $T = \infty$ $(T = 0)$.

$S_0 = \ln(40)$ towards the high-temperature limit $S_\infty = \ln(120)$ [see Figs. 1(b) and 1(c)].

Comparison with the exact results shows that calculating the finite-temperature properties directly from the static partition function $Z_{\rm st}$, i.e., by taking the corresponding derivatives of $F_{\rm st} = -k_{\rm B}T \ln(Z_{\rm st})$, is a very poor approximation. As shown by Kakehashi in the low-temperature limit [54], the ground-state moment $\langle \hat{S}^2 \rangle$ is significantly underestimated. Moreover, $\langle \hat{S}^2 \rangle$ increases with increasing T, which implies that the internal energy decreases. Therefore, the method yields a negative heat capacity C for $k_{\rm B}T \lesssim 0.8J$ and a positively diverging entropy for $T \to 0$; see Figs. 1(b) and 1(c). At least in the present atomic limit, this approach is not satisfactory. Even at high temperatures (e.g., $k_{\rm B}T \gtrsim 2J$), it does not seem particularly accurate.

Remarkably, the previous serious drawbacks are not a consequence of the static approximation itself, i.e., they are not inherent to the static description of spin fluctuations. Indeed, the local moment $\langle \hat{S}^2 \rangle$ and its Cartesian components

calculated by using the static density operator $\hat{\rho}_{st}$ are very close to the exact results for all temperatures [see Fig. 1(a)]. Notice, moreover, that this approximation respects the spin-rotational symmetry on average, since $\langle \hat{S}_z^2 \rangle = \langle \hat{S}_y^2 \rangle = \langle \hat{S}_x^2 \rangle = \langle \hat{S}^2 \rangle / 3$. As shown in Fig. 1(b), very good results are also found for the heat capacity $C_{\rm st}$, as obtained either from the temperature dependence of the average energy [Eq. (24)] or from the energy fluctuations [Eq. (25)]. It should be noted, however, that the latter tends to overestimate C and is thus somewhat less accurate [see Fig. 1(b)]. This is understandable since the variance of the energy involves a higher level of correlations than the energy itself.

Finally, the approximations to the entropy $S_{\rm st}$, calculated by integrating $C_{\rm st}/T$ as a function of T, are also very good. On the one side, starting the integration from $T = 0$ [dash-dotted curve in Fig. 1(c)], one obtains quantitatively accurate results for $k_{\rm B}T \lesssim J/2$ and a systematic overestimation of about 5–7% for large T. On the other side, starting from $\beta = 0$ [full curve in Fig. 1(c)], $S_{\rm st}$ matches the exact solution remarkably well, except for $k_{\rm B}T \lesssim J/2$ where an underestimation by less than 4% is obtained. The quality of the results for $S_{\rm st}$ might seem expected in view of the correctness of $C_{\rm st}$. Still, this actually shows that calculating $S[\hat{\rho}_{\rm st}]$ by integrating the heat capacity $C_{\rm st}$ is a very useful approach. In the anisotropic case, however, the approximation breaks down at very low temperatures, as will be discussed below.

In sum, the results for the isotropic model demonstrate that the static density operator $\hat{\rho}_{\rm st}$ provides a physically sound and quantitatively accurate description of the finite-temperature equilibrium state. This constitutes a significant improvement with respect to previous formulations based on straightforward derivations of the logarithm of the static partition function $Z_{\rm st}$.

B. Anisotropic case

While spin-rotational-invariant theories of magnetism are required to perform well in an isotropic environment, it is equally important to aim for an accurate description of the response to symmetry-breaking perturbations. The local magnetic field B considered in the present model may correspond to a uniform external field or to a local anisotropy field, which simulates the effects of spin-orbit interactions. In Figs. 2 and 3, we consider $B = 0.01J$ as a first representative example, where J refers to the exchange integral. Assuming that $J \simeq 0.7$–1.0 eV, as typically found in $3d$ transition metals, this would represent an exceptionally strong external $B \simeq 120$–170 T or a very large magnetic anisotropy energy $\Delta E \simeq 7$–10 meV/atom, sometimes reached in ultrathin films, nanowires, or small clusters. Results for other values of B are discussed below.

Two distinct temperature regimes need to be distinguished. For not-too-low T (i.e., $T/J > 0.1$ or $T/B > 10$), the thermodynamic properties are qualitatively very similar to the isotropic case. The drawbacks of previous static approaches remain, while the results derived from the static density operator $\hat{\rho}_{\rm st}$ are all in very good agreement with the exact solution (see Fig. 2). The low-temperature regime displayed in Fig. 3 is certainly more challenging, since it is comprised of the crossover from a uniaxial ground state to the isotropic behavior. The temperature here is comparable to the field-induced multiplet splitting. In this range, the total local moment $\langle \hat{S}^2 \rangle$ remains at the ground-state value, since it is governed by the much larger exchange energy J. This is very accurately reproduced by $\langle \hat{S}^2 \rangle_{\rm st}$, as obtained from $\hat{\rho}_{\rm st}$, but not by the corresponding derivative of $F_{\rm st}$. The spin magnetization $\langle \hat{S}_z \rangle$ induced by B decreases with increasing T, from the saturated ground-state value $S_z = 3/2$ to $S_z \simeq 0$ for $T/J \simeq 0.1$ ($T/B \simeq 10$). At the same time, the longitudinal (transversal) component $\langle \hat{S}_z^2 \rangle$ ($\langle \hat{S}_\rho^2 \rangle = \langle \hat{S}_x^2 + S_y^2 \rangle$) of the local moments decreases (increases), attaining $\langle \hat{S}^2 \rangle / 3$ ($2\langle \hat{S}^2 \rangle / 3$) already for $T/J \simeq 0.05$ or, equivalently, $T/B \simeq 5$. This crossover to the isotropic regime is well described in our approximation [see Fig. 3(a)]. However, notice that $\langle \hat{S}_z^2 \rangle$ ($\langle \hat{S}_\rho^2 \rangle$) is underestimated (overestimated). In fact, $\hat{\rho}_{\rm st}$ exaggerates the temperature dependence of $\langle \hat{S}_z \rangle$, $\langle \hat{S}_z^2 \rangle$, and $\langle \hat{S}_\rho^2 \rangle$ at very low temperatures. It predicts a linear temperature dependence where the exact changes are exponentially small. The linear

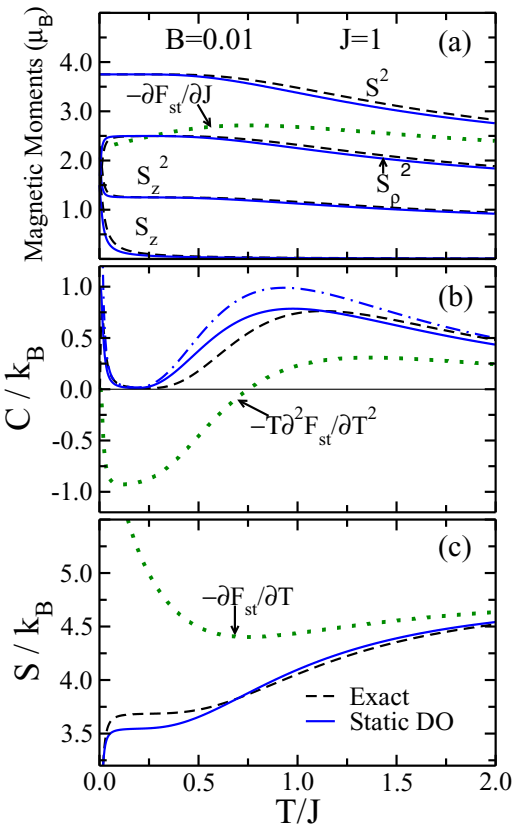

FIG. 2. Thermodynamic properties of the single-site model in a local magnetic field $B = 0.01J$, where J is the intra-atomic exchange integral: (a) Spin magnetization $\langle \hat{S}_z \rangle$, total local moment $S^2 = \langle \hat{S}_\rho^2 + Sz^2 \rangle$, longitudinal component $\langle \hat{S}_z^2 \rangle$, and transversal component $\langle \hat{S}_\rho^2 \rangle = \langle \hat{S}_x^2 + S_y^2 \rangle$, (b) heat capacity C, and (c) entropy S as a function of temperature T. The full blue curves are obtained by averaging with the static density operator $\hat{\rho}_{\rm st}$ [Eq. (20)], the dashed black curves are exact results, and the dotted green curves result from the derivatives of the static free energy $F_{\rm st}$ [Eqs. (12)–(16)]. In (b), the full and dash-dotted blue curves correspond to Eqs. (24) and (25), respectively. In (c), the full (dash-dotted) blue curve is obtained by integrating $C_{\rm st}/T$ starting from $T = \infty$ ($T = 0$). The low-temperature regime is highlighted in Fig. 3.

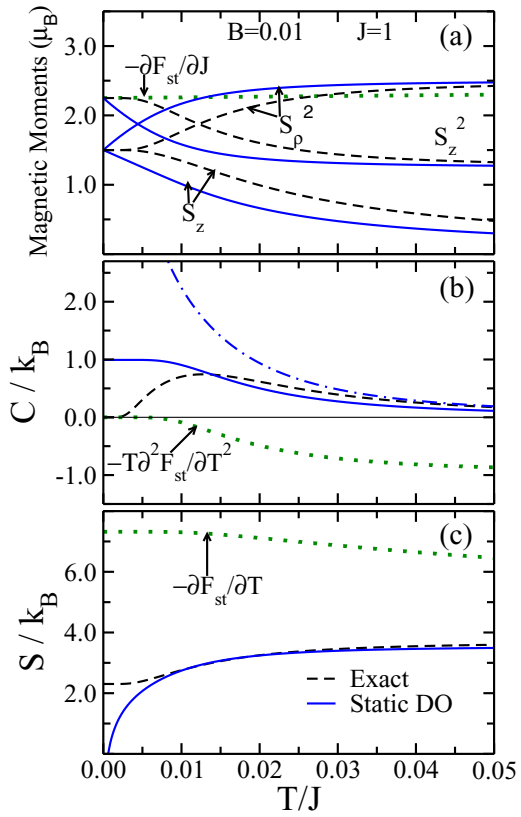

FIG. 3. Low-temperature thermodynamic properties of the single-site model in a local magnetic field $B = 0.01J$, where J is the intra-atomic exchange integral: (a) Spin magnetization $\langle \hat{S}_z \rangle$, total local moment $S^2 = \langle \hat{S}_\rho^2 + Sz^2 \rangle$, longitudinal component $\langle \hat{S}_z^2 \rangle$, and transversal component $\langle \hat{S}_\rho^2 \rangle = \langle \hat{S}_x^2 + S_y^2 \rangle$, (b) heat capacity C, and (c) entropy S. All model parameters and curve styles are the same as in Fig. 2.

decrease of $\langle \hat{S}_z \rangle_{st}$ also affects the temperature dependence of the average energy E and its fluctuations. This leads to inaccuracies in the specific heat and entropy for $T \to 0$, which are discussed below. The static approximation, therefore, fails to accurately reproduce the thermal activation across the discrete spectrum of the single-site model (finite gap of the order of B). Even so, this problem is expected to become less important as the system size increases and in the macroscopic limit.

In Fig. 3(b), results are given for the heat capacity C as a function of T. As in the isotropic case, the values obtained from the second derivative of F_{st} are negative. The approximations C_{st} and C'_{st} which are obtained using $\hat{\rho}_{st}$ from the temperature dependence of the average energy and its fluctuations [Eqs. (24) and (25)] are very close to the exact solution for $T/B \gtrsim 1$ and $T/B \gtrsim 3$, respectively. However, some significant deviations appear again in the limit $T \to 0$ [see Fig. 3(b)]. On the one side, C_{st} remains essentially at a constant finite value for $T/B < 1$. This reflects the already discussed linear decrease of $\langle \hat{S}_z \rangle_{st}$ with increasing T. Far more dramatic are the results for $C'_{st} = \Delta E^2/T^2$, deduced from the average energy fluctuations $\Delta E^2 = \langle \hat{H}^2 \rangle_{st} - \langle \hat{H} \rangle_{st}^2$. Although ΔE^2 converges properly to zero, as expected, the dependence on T is only linear. This is obviously too slow and leads to a $1/T$ divergence of C'_{st}. The breakdown of C'_{st} in the low-temperature limit is probably understandable since ΔE^2 involves higher-order correlations, which are difficult to describe with the static linear decoupling.

The temperature dependence of the entropy S is shown in Fig. 3(c). For $T/J \geqslant 0.01$ ($T/B \geqslant 1$), the results obtained by integrating C_{st}/T' from $T' = \infty$ to T are remarkably close to the exact solution. However, S_{st} diverges as $\ln(T)$ in the low-temperature limit [see Fig. 3(c)]. This is not surprising since $S_{st} \propto \ln(T)$ is equivalent to the above-discussed result that C_{st} tends to a finite constant for $T \to 0$ [see Fig. 3(c)]. It is important to remark that this anomalous behavior is not an intrinsic limitation of $\hat{\rho}_{st}$. It is a consequence of the approximation used to compute S_{st}, which is based on a relation between S and C that is not valid in general. The entropy $S[\hat{\rho}_{st}] = -\langle \ln(\hat{\rho}_{st}) \rangle$ is actually a fundamental property of the mixed state $\hat{\rho}_{st}$, to be computed independently from $E = \langle \hat{H} \rangle_{st}$. In fact, it is easy to see that $S[\hat{\rho}_{st}] \to \ln(n_g)$ for $T \to 0$, where $n_g \geqslant 1$ is the degeneracy of the Hartree-Fock ground state, in which the exchange field $\vec{\xi}_0$ points along the magnetic field $\vec{B}$.

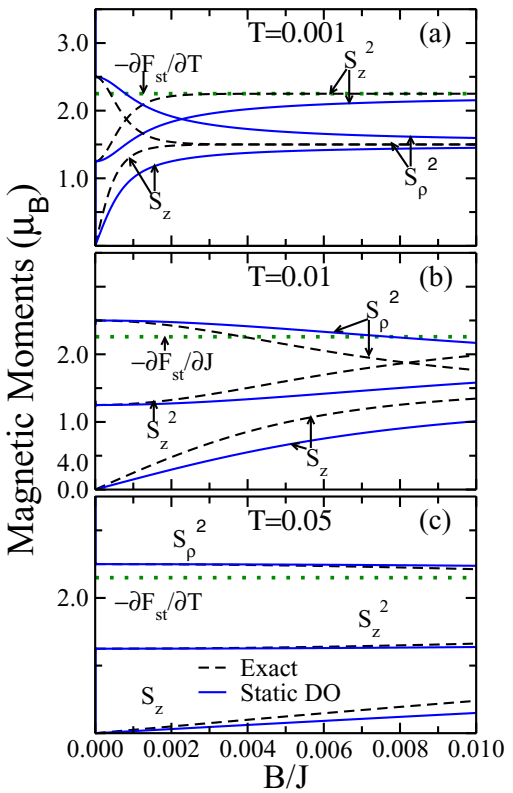

FIG. 4. Average spin magnetization $\langle \hat{S}_z \rangle$, longitudinal component $\langle \hat{S}_z^2 \rangle$, and transversal component $\langle \hat{S}_\rho^2 \rangle = \langle \hat{S}_x^2 + \hat{S}_y^2 \rangle$ of the local magnetic moments $\langle \hat{S}^2 \rangle = \langle \hat{S}_\rho^2 + \hat{S}_z^2 \rangle$ as a function of magnetic field B. The temperatures are (a) $T = 0.001J/k_B$, (b) $T = 0.01J/k_B$, and (c) $T = 0.05J/k_B$, where J stands for the intra-atomic exchange integral. The full blue curves are obtained by using the static density operator $\hat{\rho}_{st}$ [Eq. (20)], while the dashed black curves are the corresponding exact results. The green dotted curves show $\partial F_{st}/\partial J$. The total local moment $S^2 = \langle \hat{S}_\rho^2 + \hat{S}z^2 \rangle$ (not shown) remains almost exactly equal to its zero-field ground-state value $S^2 = 15/4$ for all considered B.

In Fig. 4, the spin magnetization and the local magnetic moments are shown as a function of the external magnetic field B, for three representative temperatures. As expected, the total moments $\langle \hat{S}^2 \rangle$ are not affected by changes in B, unless B and T are unreasonably high. As in previous cases, the results for $\langle \hat{S}^2 \rangle_{st}$ obtained from ρ_{st} coincide with the exact ones. Starting from the isotropic case ($B = 0$), the longitudinal component of the moment $\langle \hat{S}_z^2 \rangle$ increases at the expense of the transversal contribution $\langle \hat{S}_\rho^2 \rangle$. For low temperatures [e.g., $T/J = 0.001$ in Fig. 4(a)], saturation is almost reached for the largest considered fields (i.e., $\langle \hat{S}_z \rangle = 3/2$ and $\langle \hat{S}_z^2 \rangle = 9/4$). Notice that the response to the magnetic field is, in general, underestimated by ρ_{st}. In particular, the approach to saturation is slower than in the exact solution. Although the calculated $\langle \hat{S}_z^2 \rangle_{st}$ and $\langle \hat{S}_z \rangle_{st}$ are exact for $B = 0$, the zero-field susceptibility $\chi = (\partial \langle \hat{S}_z \rangle / \partial B)_{B=0}$ is underestimated by 40% (see Fig. 4). This discrepancy is due to the fact that $\hat{S}_z$ does not commute with the effective single-particle Hamiltonian $\hat{H}'(\vec{\xi})$, even though it commutes with $\hat{H}$ [compare Eqs. (2) and (10)]. As a result, $(\partial \langle \hat{S}_z \rangle_{st} / \partial B)$ does not coincide with $\chi = (\langle \hat{S}_z^2 \rangle_{st} - \langle \hat{S}_z \rangle_{st}^2)/T$ as in the exact case [see Eq. (19)]. If we use the latter expression for χ, our results are essentially exact.

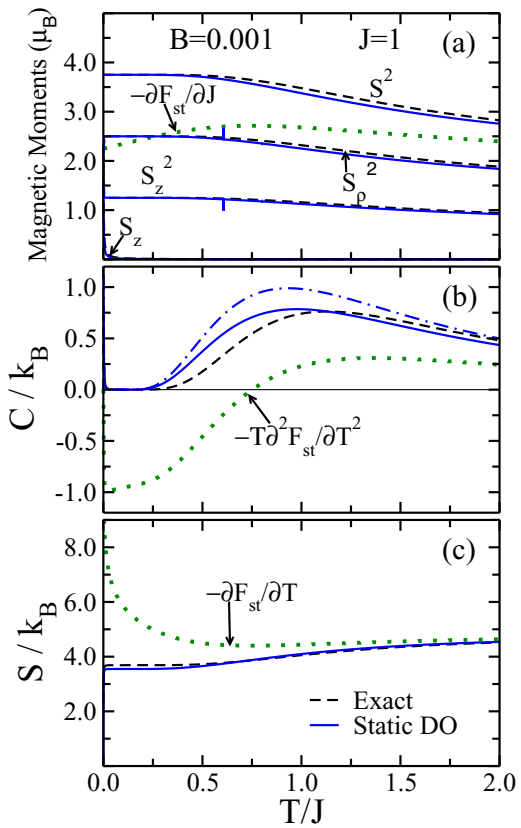

FIG. 5. Thermodynamic properties of the single-site model in a local magnetic field $B = 0.001J$, where J is the intra-atomic exchange integral: (a) Spin magnetization $\langle \hat{S}_z \rangle$, total local moment $S^2 = \langle \hat{S}_\rho^2 + Sz^2 \rangle$, longitudinal component $\langle \hat{S}_z^2 \rangle$, and transversal component $\langle \hat{S}_\rho^2 \rangle = \langle \hat{S}_x^2 + S_y^2 \rangle$, (b) heat capacity C, and (c) entropy S. The style assigned to each curve is the same as in Fig. 2. The low-temperature regime is highlighted in Fig. 6.

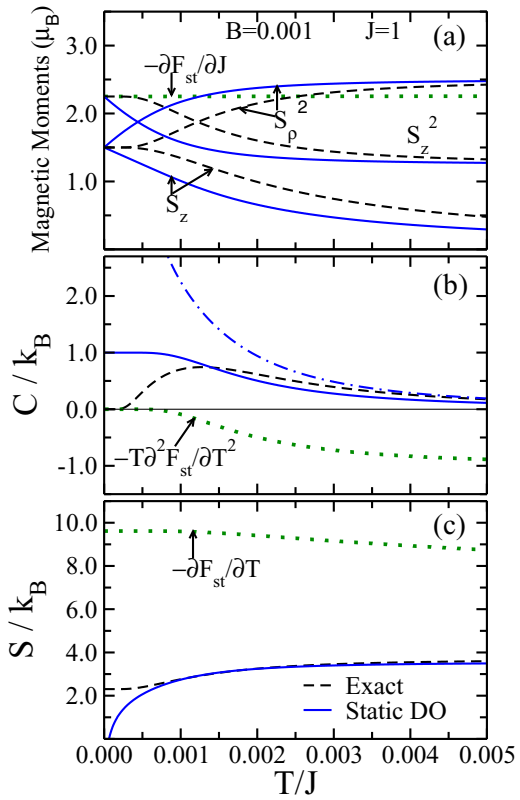

FIG. 6. Low-temperature thermodynamic properties of the single-site model in a local magnetic field $B = 0.001J$, where J is the intra-atomic exchange integral: (a) Spin magnetization $\langle \hat{S}_z \rangle$, total local moment $S^2 = \langle \hat{S}_\rho^2 + Sz^2 \rangle$, longitudinal component $\langle \hat{S}_z^2 \rangle$, and transversal component $\langle \hat{S}_\rho^2 \rangle = \langle \hat{S}_x^2 + S_y^2 \rangle$, (b) heat capacity C, and (c) entropy S. All model parameters and curve styles are the same as in Fig. 5.

Before closing this section, we would like to briefly discuss the temperature dependence of the thermodynamic properties of the model for two additional values of B/J. As already discussed, the results shown in Figs. 2 and 3 for $B = 0.01J$ correspond to a very strong external or local anisotropy field, assuming that $J \simeq 0.7$–1.0 eV is appropriate for $3d$ transition metals. It is therefore interesting to also consider smaller fields, for example, $B = 0.001J$ as shown in Fig. 5. For not-too-low T, one observes that the temperature dependence of all considered properties is very similar to the isotropic case (Fig. 1). Of course, this does not hold at low T (i.e., for $T \lesssim 5B$) where the differences between isotropic and anisotropic cases are always qualitatively important. The more challenging low-temperature regime is highlighted in Fig. 6. In this case, we find essentially the same behavior as for $B = 0.01J$ but in an accordingly scaled temperature range (compare Figs. 3 and 6). This could have been expected since for $J \gg B,T$ only the lowest-S multiplet matters (in the present case, $S = 3/2$) and therefore the temperature dependence scales with T/B.

Perhaps more of a theoretical curiosity, at least at first sight, is the case of an even larger local magnetic field, for example, $B = 0.1J$, as shown in Fig. 7. Indeed, such values of B are certainly unattainable, either as external or as local

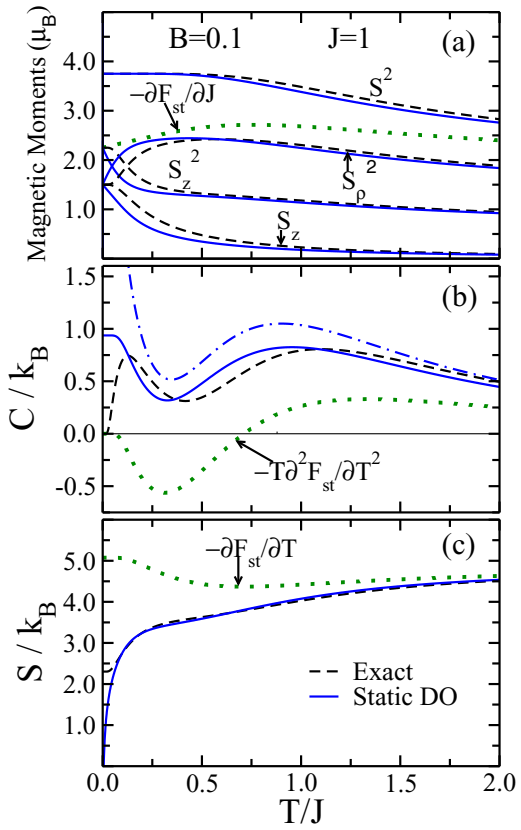

FIG. 7. Thermodynamic properties of the single-site model in a local magnetic field $B = 0.1J$, where J is the intra-atomic exchange integral: (a) Spin magnetization $\langle \hat{S}_z \rangle$, total local moment $S^2 = \langle \hat{S}_\rho^2 + Sz^2 \rangle$, longitudinal component $\langle \hat{S}_z^2 \rangle$, and transversal component $\langle \hat{S}_\rho^2 \rangle = \langle \hat{S}_x^2 + S_y^2 \rangle$, (b) heat capacity C, and (c) entropy S. The style assigned to each curve is the same as in Fig. 2.

anisotropy fields, if one presupposes that J corresponds to $3d$ transition metals. Nevertheless, the results still seem of interest in order to complete the assessment of the different approximations or as a possibility of modeling systems with a weak exchange interaction J. The results show that averaging with $\hat{\rho}_{st}$ remains a very effective method of calculating the temperature-dependent properties, even for very large fields. This holds, in particular, for the local magnetic moments, their longitudinal and transversal components and the field-induced magnetization [Fig. 7(a)]. Significant deviation from the exact results is only found at low temperatures. The nonmonotonous temperature dependence of the heat capacity is well reproduced by both approximations C_{st} and C'_{st}, except for $T/B \lesssim 1$, where the former remains constant, failing to tend to zero, and the latter diverges. As for the other values of B, the entropy S_{st} obtained by integrating C_{st} is remarkably accurate over a very broad temperature range, in contrast to previous approaches [see Fig. 7(c)]. Only in the limit of $T \to 0$ does the approximation for S_{st}, which consists in integrating C_{st}/T, break down since C_{st} tends to a nonzero constant and, therefore, $S_{st} \propto \ln(T)$. As already discussed, this is not a flaw of $\hat{\rho}_{st}$, which can be shown to always have a finite positive entropy $S[\hat{\rho}_{st}]$ at $T = 0$.

IV. CONCLUSION

A spin-rotational-invariant theory of finite-temperature transition-metal magnetism has been presented. Starting from a many-body model Hamiltonian for the valence $3d$ electrons, the noncollinear spin fluctuations are taken into account in the framework of the static approximation to the vector-field functional-integral method. A change of perspective to the solution of this longstanding problem is proposed. Instead of using the static assumption to calculate the partition function Z and derive the thermodynamics from the derivatives of the approximate free energy $F_{st} = -k_B \ln(Z_{st})$, we regard the Hubbard-Stratonovich transformation as an operator identity and derive a static approximation to the density operator $\hat{\rho}$ which characterizes the equilibrium mixed state. The thus obtained static density operator $\hat{\rho}_{st}$ gives us direct access to the thermodynamic averages of any observable. The following goal of this paper has been to assess the validity of the proposed method or, in other words, to judge the ability of $\hat{\rho}_{st}$ to describe the many-body equilibrium state. To this aim, the atomic limit of the model has been investigated in detail, taking Fe as a representative example. The comparison between exact and approximate results demonstrates that $\hat{\rho}_{st}$ provides a physically sound and quantitatively accurate account of the finite-temperature properties over a wide temperature range. Significant deviations from the exact behavior are only found in the entropy and heat capacity, when a local magnetic field B is present and the temperature is comparable to or smaller than the multiplet splitting (i.e., $k_B T \lesssim \mu_B B$). This is not expected to be a problem in most practical applications since the temperature equivalent of external or anisotropy magnetic fields seldom surpasses 20 K. We conclude that important progress has been achieved, particularly in comparison with previous static approaches, which yield unphysical results in the atomic limit [54]. The quantum-mechanical reasons behind these improvements have been identified. The general validity of these arguments suggests that our conclusions should also apply to more sophisticated multiband models as well as to first-principles methods.

Understanding itinerant-electron magnetism at a microscopic level represents a particularly important, yet unsolved problem in condensed-matter physics. Spin-rotational-invariant theories, incorporating longitudinal and transversal spin excitations on the same footing, are particularly appealing. They are physically far superior to broken-symmetry longitudinal models on both energetic and entropic issues. Moreover, the noncollinear point of view gives access to arbitrary complex forms of magnetic order (e.g., spin spirals, skyrmions, and other chiral structures), which are attracting considerable experimental and theoretical attention. Grasping the stability of these magnetic structures at finite temperatures and the nature of the dominant spin excitations is a fascinating challenge. Furthermore, the vector character of spin excitations is expected to be crucial for the study of subtle, symmetry-sensitive effects such as spin-orbit coupling, magnetic anisotropy, and orbital magnetism. The present work opens an alternative route to the development of noncollinear spin-fluctuation theory with a variety of interesting perspectives. Improvements on the model, which allow a more realistic description of the single-particle electronic structure,

are straightforward, in particular by including *sp* electrons and *sp-d* hybridizations. In this way, one could take advantage of the relations between the present approach and first-principles theories of finite-temperature magnetism. One may consider, for example, a tight-binding representation of the Kohn-Sham Hamiltonian, as proposed in Ref. [59], and derive the thermodynamic properties from the static approximation to $\hat{\rho}$ developed here. The operator perspective adopted in this work should also be helpful in the more general framework of finite-temperature density-functional theory [60] and in the context of dynamical approximations to the many-electron problem in narrow bands [22].

The relative simplicity of the present approach can be exploited to investigate large finite clusters, low-dimensional systems, and nanostructures. Quantum-mechanical averages can be obtained in the framework of the single-particle Hamiltonian $\hat{H}'(\vec{\xi})$ by using Green's-function methods, while statistical averages over the exchange-field configurations can be performed by Monte Carlo methods or alloy-analogy approximations. Particularly challenging are the applications to magnetic anisotropy and spin-orbit effects, whose temperature dependence remains, to a large extent, unexplored from the point of view of theory.

ACKNOWLEDGMENT

This work has been supported by the DAAD (Germany)-CONACyT (Mexico) exchange program PROALMEX.

[1] A. Fert, V. Cros, and J. Sampaio, Nat. Nanotechnol. **8**, 152 (2013); S. S. Parkin, M. Hayashi, and L. Thomas, Science **320**, 190 (2008); N. Romming, Ch. Hanneken, M. Menzel, J. E. Bickel, B. Wolter, K. von Bergmann, A. Kubetzka, and R. Wiesendanger, *ibid.* **341**, 636 (2013).

[2] A. A. Khajetoorians, M. Valentyuk, M. Steinbrecher, T. Schlenk, A. Shick, J. Kolorenc, A. I. Lichtenstein, T. O. Wehling, R. Wiesendanger, and J. Wiebe, Nat. Nanotechnol. **10**, 958 (2015).

[3] K. von Bergmann, Science **349**, 234 (2015).

[4] I. G. Rau, S. Baumann, S. Rusponi, F. Donati, S. Stepanow, L. Gragnaniello, J. Dreiser, C. Piamonteze, F. Nolting, S. Gangopadhyay, O. R. Albertini, R. M. Macfarlane, C. P. Lutz, B. A. Jones, P. Gambardella, A. J. Heinrich, and H. Brune, Science **344**, 988 (2014).

[5] G. Ju, Y. Peng, E. K. C. Chang, Y. Ding, A. Q. Wu, X. Zhu, Y. Kubota, T. J. Klemmer, H. Amini, L. Gao, Z. Fan, T. Rausch, P. Subedi, M. Ma, S. Kalarickal, C. J. Rea, D. V. Dimitrov, P.-W. Huang, K. Wang, X. Chen, C. Peng, W. Chen, J. W. Dykes, M. A. Seigler, E. C. Gage, R. Chantrell, and J.-U. Thiele, IEEE Trans. Magn. **51**, 3201709 (2015).

[6] F. Donati, Q. Dubout, G. Autes, F. Patthey, F. Calleja, P. Gambardella, O. V. Yazyev, and H. Brune, Phys. Rev. Lett. **111**, 236801 (2013).

[7] A. Sonntag, J. Hermenau, A. Schlenhoff, J. Friedlein, S. Krause, and R. Wiesendanger, Phys. Rev. Lett. **112**, 017204 (2014).

[8] A. A. Khajetoorians, M. Steinbrecher, M. Ternes, M. Bouhassoune, M. dos Santos Dias, S. Lounis, J. Wiebe, and R. Wiesendanger, Nat. Commun. **7**, 10620 (2016).

[9] C. Boeglin, E. Beaurepaire, V. Halté, V. López-Flores, C. Stamm, N. Pontius, H. A. Durr, and J.-Y. Bigot, Nature (London) **465**, 458 (2010); E. Turgut, C. La-o-vorakiat, J. M. Shaw, P. Grychtol, H. T. Nembach, D. Rudolf, R. Adam, M. Aeschlimann, C. M. Schneider, T. J. Silva, M. M. Murnane, H. C. Kapteyn, and S. Mathias, Phys. Rev. Lett. **110**, 197201 (2013); B. Koopmans, H. H. J. E. Kicken, M. van Kampen, and W. J. M. de Jonge, J. Magn. Magn. Mater. **286**, 271 (2005); C. Stamm, T. Kachel, N. Pontius, R. Mitzner, T. Quast, K. Holldack, S. Khan, C. Lupulescu, E. F. Aziz, M. Wietstruk, H. A. Durr, and W. Eberhardt, Nat. Mater. **6**, 740 (2007).

[10] D. Steiauf and M. Fähnle, Phys. Rev. B **79**, 140401 (2009).

[11] W. Töws and G. M. Pastor, Phys. Rev. Lett. **115**, 217204 (2015).

[12] M. Dantziger, B. Glinsmann, S. Scheffler, B. Zimmermann, and P. J. Jensen, Phys. Rev. B **66**, 094416 (2002).

[13] J. C. Neto, J. R. de Sousa, and J. A. Plascak, Phys. Rev. B **66**, 064417 (2002).

[14] M. Pajda, J. Kudrnovský, I. Turek, V. Drchal, and P. Bruno, Phys. Rev. Lett. **85**, 5424 (2000); Phys. Rev. B **64**, 174402 (2001).

[15] T. Herrmann, M. Potthoff, and W. Nolting, Phys. Rev. B **58**, 831 (1998); J. H. Wu, H. Y. Chen, and W. Nolting, *ibid.* **65**, 014424 (2001),

[16] P. Bruno, Phys. Rev. Lett. **87**, 137203 (2001).

[17] M. Y. Lavrentiev, R. Soulairol, C.-C. Fu, D. Nguyen-Manh, and S. L. Dudarev, Phys. Rev. B **84**, 144203 (2011).

[18] F. López-Urías. G. M. Pastor and K. H. Bennemann, J. Appl. Phys. **87**, 4909 (2000).

[19] H. Hasegawa, J. Phys. F: Metal Phys. **16**, 347 (1986); **17**, 165 (1987); Surf. Sci. **182**, 591 (1987); J. Phys.: Condens. Matter **1**, 9325 (1989).

[20] J. B. Staunton and B. L. Gyorffy, Phys. Rev. Lett. **69**, 371 (1992); S. S. A. Razee, J. B. Staunton, L. Szunyogh, and B. L. Györffy, Phys. Rev. B **66**, 094415 (2002); J. B. Staunton, S. Ostanin, S. S. A. Razee, B. L. Györffy, L. Szunyogh, B. Ginatempo, and Ezio Bruno, Phys. Rev. Lett. **93**, 257204 (2004); J. B. Staunton, L. Szunyogh, A. Buruzs, B. L. Györffy, S. Ostanin, and L. Udvardi, Phys. Rev. B **74**, 144411 (2006).

[21] I. A. Zhuravlev and V. P. Antropov, and K. D. Belashchenko, Phys. Rev. Lett. **115**, 217201 (2015).

[22] A. I. Lichtenstein, M. I. Katsnelson, and G. Kotliar, Phys. Rev. Lett. **87**, 067205 (2001).

[23] G. M. Pastor, J. Dorantes-Dávila, and K. H. Bennemann, Phys. Rev. B **70**, 064420 (2004).

[24] R. Garibay-Alonso, J. Dorantes-Dávila, and G. M. Pastor, Phys. Rev. B **73**, 224429 (2006).

[25] R. Garibay-Alonso, J. Dorantes-Dávila, and G. M. Pastor, Phys. Rev. B **79**, 134401 (2009).

[26] R. Garibay-Alonso, J. Dorantes-Dávila, and G. M. Pastor, Phys. Rev. B **85**, 224409 (2012).

[27] Y. Kakehashi, J. Phys. Soc. Jpn. **50**, 2251 (1981).

[28] Peter Fulde, *Electron Correlations in Molecules and Solids*, Springer Series in Solid State Sciences (Springer-Verlag, Berlin, 1991), Vol. 100.

[29] I. A. Abrikosov, A. V. Ponomareva, P. Steneteg, S. A. Barannikova, and B. Alling, Curr. Opin. Solid State Mater. Sci. **20**, 85 (2016).
[30] T. Oda, A. Pasquarello, and R. Car, Phys. Rev. Lett. **80**, 3622 (1998).
[31] P. Bobadova-Parvanova, K. A. Jackson, S. Srinivas, and M. Horoi, Phys. Rev. A **67**, 061202(R) (2003).
[32] D. Hobbs, G. Kresse, and J. Hafner, Phys. Rev. B **62**, 11556 (2000).
[33] N. O. Jones, S. N. Khanna, T. Baruah, and M. R. Pederson, Phys. Rev. B **70**, 045416 (2004).
[34] T. Morisato, S. N. Khanna, and Y. Kawazoe, Phys. Rev. B. **72**, 014435 (2005).
[35] R. C. Longo, E. G. Noya, and L. J. Gallego, J. Chem. Phys. **122**, 226102 (2005); Phys. Rev. B **72**, 174409 (2005).
[36] M. Kabir, A. Mookerjee and D. G. Kanhere, Phys. Rev. B **73**, 224439 (2006); M. Kabir, D. G. Kanhere, and A. Mookerjee, *ibid.* **75**, 214433 (2007).
[37] R. C. Longo, M. M. G. Alemany, J. Ferrer, A. Vega, and L. J. Gallego, J. Chem. Phys. **128**, 114315 (2008).
[38] M. A. Ojeda, J. Dorantes-Dávila, and G. M. Pastor, Phys. Rev. B **60**, 6121 (1999).
[39] P. Ruiz-Díaz, R. Garibay-Alonso, J. Dorantes-Dávila, and G. M. Pastor, Phys. Rev. B **84**, 024431 (2011).
[40] M. Saubanère, M. Tanveer, P. Ruiz-Díaz, and G. M. Pastor, Phys. Status Solidi B **247**, 2610 (2010).
[41] J. C. Tung and G. Y. Guo, Phys. Rev. B **83**, 144403 (2011).
[42] F. Schubert, Y. Mokrousov, P. Ferriani, and S. Heinze, Phys. Rev. B **83**, 165442 (2011).
[43] M. Tanveer, P. Ruíz-Díaz, and G. M. Pastor, Phys. Rev. B **87**, 075426 (2013).
[44] H. Ebert and S. Mankovsky, Phys. Rev. B **79**, 045209 (2009).
[45] Y. Kakehashi, Phys. Rev. B **65**, 184420 (2002).
[46] Y. Kakehashi, T. Shimabukuro, T. Tamashiro, and T. Nakamura, J. Phys. Soc. Jpn. **77**, 094706 (2008).
[47] Y. Kakehashi and M. A. R. Patoary, Phys. Rev. B **83**, 144409 (2011).
[48] R. Garibay-Alonso, J. Dorantes-Dávila, and G. M. Pastor, Phys. Rev. B **91**, 184408 (2015).
[49] J. Hubbard, Phys. Rev. B **19**, 2626 (1979); **20**, 4584 (1979).
[50] M. V. You and V. Heine, J. Phys. F: Met. Phys. **12**, 177 (1982).
[51] M. Uhl and J. Kübler, Phys. Rev. Lett. **77**, 334 (1996).
[52] B. S. Pujari, P. Larson, V. P. Antropov, and K. D. Belashchenko, Phys. Rev. Lett. **115**, 057203 (2015).
[53] T. Uchida and Y. Kakehashi, Phys. Rev. B **64**, 054402 (2001).
[54] Y. Kakehashi, Phys. Rev. B **31**, 3104 (1985).
[55] Calculations reported in this paper were performed using MATHEMATICA, version 10.0, computer software (Wolfram Research, Inc., Champaign, IL, 2014).
[56] R. L. Stratonovich, Dokl. Akad. Nauk SSSR **115**, 1097 (1957) [Sov. Phys. Dokl. **2**, 416 (1958)]; J. Hubbard, Phys. Rev. Lett. **3**, 77 (1959).
[57] R. P. Feynman, Phys. Rev. **84**, 108 (1951).
[58] See Supplemental Material at http://link.aps.org/supplemental/10.1103/PhysRevB.93.214435 where analytic expressions for the heat capacity in two different approximations are given.
[59] O. K. Andersen and O. Jepsen, Phys. Rev. Lett. **53**, 2571 (1984).
[60] N. D. Mermin, Phys. Rev. **137**, A1441 (1965).